On the communication over strong atmospheric turbulence channels by adaptive modulation and coding

Ivan B. Djordjevic[1*] and Goran T. Djordjevic[2]

[1]*Department of Electrical and Computer Engineering, University of Arizona, Tucson, AZ 85721, USA*
[2]*University of Nis, Faculty of Electronic Engineering, Nis 18000, Serbia*
**ivan@ece.arizona.edu*

Abstract: The free-space optical (FSO) communications can provide any connectivity need at high-speed. However, an optical wave propagating through the atmosphere experiences the variation in amplitude and phase due to scintillation. To enable high-speed communication over strong atmospheric turbulence channels, we propose to transmit the encoded sequence over both FSO and wireless channels, feedback channel state information of both channels by RF-feedback, and adapt powers and rates so that total channel capacity is maximized. The optimum power adaptation policy maximizing total channel capacity is derived. We show significant spectral efficiency performance improvement by employing this approach. We further show that deep fades in the order 35 dB and above can be tolerated by proposed hybrid communication scheme.

OCIS codes: (010.1330) Atmospheric turbulence; (060.2605) Free-space optical communication; (060.4080) Modulation.

References and links

1. L. C. Andrews, and R. L. Philips, *Laser Beam Propagation through Random Media* (SPIE Press, 2005).
2. I. B. Djordjevic, B. Vasic, and M. A. Neifeld, "LDPC coded OFDM over the atmospheric turbulence channel," Opt. Express **15**, 6332–6346 (2007).
3. I. B. Djordjevic, S. Denic, J. Anguita, B. Vasic, and M. A. Neifeld, "LDPC-coded MIMO optical communication over the atmospheric turbulence channel," J. Lightwave Technol. **26**(5), 478–487 (2008).
4. J. A. Anguita, M. A. Neifeld, B. Hildner, and B. Vasic, "Raptor codes for the temporally correlated FSO channel," submitted for publication.
5. S. Denic, I. B. Djordjevic, J. Anguita, B. Vasic, and M. A. Neifeld, "Information theoretic limits for free-space optical channels with and without memory," J. Lightwave Technol. **26**(19), 3376–3384 (2008).
6. A. Goldsmith, *Wireless Communications* (Cambridge University Press, Cambridge 2005).
7. A. Goldsmith, and S.-G. Chua, "Adaptive coded modulation for fading channels," IEEE Trans. Commun. **46**(5), 595–602 (1998).
8. M. D. Yacoub, "The α-μ distribution: a general fading distribution," in Proc. IEEE Int. Symp. PIMRC, vol. 2, pp. 629–633, 2002.
9. M. D. Yacoub, "The α-μ distribution: a physical fading model for the Stacy distribution," IEEE Trans. Vehicular Technol. **56**(1), 27–34 (2007).
10. M. A. Al-Habash, L. C. Andrews, and R. L. Phillips, "Mathematical model for the irradiance probability density function of a laser beam propagating through turbulent media," Opt. Eng. **40**(8), 1554–1562 (2001).
11. J. A. Anguita, I. B. Djordjevic, M. A. Neifeld, and B. V. Vasic, "Shannon capacities and error–correction codes for optical atmospheric turbulent channels," J. Opt. Netw. **4**(9), 586–601 (2005).
12. M. P. C. Fossorier, "Quasi-cyclic low-density parity-check codes from circulant permutation matrices," IEEE Trans. Inf. Theory **50**(8), 1788–1793 (2004).
13. H. Xiao-Yu, E. Eleftheriou, D.-M. Arnold, and A. Dholakia, "Efficient implementations of the sum-product algorithm for decoding of LDPC codes," In Proc. IEEE Globecom 2001, vol. 2, pp. 1036–1036E, 2001.
14. T. Mizuochi, Y. Miyata, T. Kobayashi, K. Ouchi, K. Kuno, K. Kubo, K. Shimizu, H. Tagami, H. Yoshida, H. Fujita, M. Akita, and K. Motoshima, "Forward error correction based on block turbo code with 3-bit soft decision for 10-Gb/s optical communication systems," IEEE J. Sel. Top. Quantum Electron. **10**(2), 376–386 (2004).
15. A. A. Farid, and S. Hranilovic, "Upper and lower bounds on the capacity of wireless optical intensity channels," in Proc. ISIT 2007, pp. 2416–2420, Nice, France, June 24-June 29, 2007.

#113782 - $15.00 USD Received 6 Jul 2009; revised 28 Aug 2009; accepted 10 Sep 2009; published 25 Sep 2009

1. Introduction

Free-space optical (FSO) communications can address any connectivity need in future optical networks [1]. In metropolitan area networks (MANs), the FSO communication systems can be used to extend the existing MAN rings; in enterprise, the FSO systems can be used to provide local area network (LAN)-to-LAN connectivity and intercampus connectivity; and the FSO communication is an excellent candidate for the last-mile connectivity. Unfortunately, an optical wave propagating through the atmosphere experiences the fluctuations in amplitude and phase due to scintillation, which represents one of the most important factors to degrade the performance of an FSO communication system. Recently there have been proposed many different coding approaches to deal with scintillation including: coded orthogonal frequency division multiplexing (OFDM) [2], coded multi-input multi-output (MIMO) [3], and rate-less coding [4]. However, the achievable information rates (lower bounds on channel capacity) results reported in [3,5], indicate that those approaches are still several dBs away from the channel capacity, suggesting that there still exists some space for improvement.

In this paper we propose to use a hybrid FSO-RF system with adaptive modulation and coding as an efficient way to deal with strong atmospheric turbulence. Adaptive modulation and coding [6,7] can enable robust and spectrally-efficient transmission over both α-μ (or generalized Gamma) wireless fading channel and FSO channel. The key idea behind our proposal is to split the encoded sequence between FSO and wireless channels, estimate the channel conditions in both channels at the receiver side and feed this channel estimate back to both RF and FSO transmitters using an RF feedback channel, so that the transmitters can be adapted relative to the channel conditions. The power and data rate in both channels are adapted so that the total spectral efficiency in both channels is maximized. The optimum power adaptation policy is determined that maximizes channel capacity simultaneously in both channels.

The paper is organized as follows. In Section 2 we describe proposed hybrid FSO-RF system with adaptive modulation and coding, and corresponding channel models. The non-adaptive coded modulation is described in Section 3. In Section 4 we derive the optimum adaptive-power adaptive-rate adaptation policy. The adaptive coded modulation is described in Section 5. Some important concluding remarks are given in Section 6.

2. Description of system and channel models

In this section we describe the proposed system (subsection A), wireless channel model (subsection B), and FSO channel model (subsection C).

2.1 System description

The adaptive hybrid FSO-RF communication system, shown in Fig. 1, consists of two parallel FSO and RF channels. The encoded data stream is partially transmitted over FSO and partially over RF channel. Operating symbol rate of FSO channel is commonly many times higher that that of RF channel. FSO channel comprises an FSO transmitter, propagation path through the atmosphere, and an FSO receiver. The optical transmitter includes a semiconductor laser of high launch power, adaptive mapper, and power control block. To reduce the system cost, the direct modulation of laser diode is used.

The modulated beam is projected toward the distant receiver by using an expanding telescope assembly. Along the propagation path through the atmosphere, the light beam experiences absorption, scattering and atmospheric turbulence, which cause attenuation, and random variations in amplitude and phase. At the receiver side, an optical system collects the incoming light and focuses it onto a detector, which generates an electrical current proportional to the incoming power. The RF channel comprises adaptive RF mapper, RF power control, RF transmitter (Tx), transmitting antenna, wireless propagation path, receiver antenna, and RF receiver (Rx).

The RF channel estimates and FSO irradiance estimates are transmitted back to transmitters using the same RF feedback channel. Because the atmospheric turbulence

#113782 - $15.00 USD Received 6 Jul 2009; revised 28 Aug 2009; accepted 10 Sep 2009; published 25 Sep 2009

changes slowly, with correlation time ranging from 10 μs to 10 ms, this is a plausible scenario for FSO channels with data rates in the order of Gb/s. Notice that erbium doped fiber amplifiers (EDFAs) cannot be used at all in this scenario because the fluorescence time is too long (about 10 ms). The semiconductor optical amplifiers (SOAs) should be used instead, if needed. The data rates and powers in both channels are varied in accordance with channel conditions. The symbol rates on both channels are kept fixed while the signal constellation diagrams sizes are varied based on channel conditions. When FSO (RF) channel condition is favorable larger constellation size is used, when FSO (RF) channel condition is poor smaller constellation size is used, and when the FSO (RF) channel signal-to-noise ratio (SNR) falls below threshold the signal is not transmitted at all. Both subsystems (FSO and RF) are designed to achieve the same target bit error probability (P_b). The RF subsystem employs M-ary quadrature amplitude modulation (MQAM), while FSO subsystem employs the M-ary pulse amplitude modulation (MPAM). MPAM is selected for FSO subsystem because negative amplitude signals cannot be transmitted over FSO channels with direct detection. These two modulation formats are selected as an illustrative example; the proposed scheme, however, is applicable to arbitrary multilevel modulations. The optimum variable-power variable-rate policy, maximizing total channel capacity, is described in Section 4. In the rest of this section we describe the wireless and the FSO channel models. Both RF and FSO channels are modeled as *block-fading* channels, because symbol durations in both channels are much shorter than the corresponding coherence times. The duration of the block is proportional to the coherence time of the channel, which is from 10 μs-10 ms for FSO channel and from 10 ms-1 s for RF channels. We therefore assume the i.i.d. fading between the blocks.

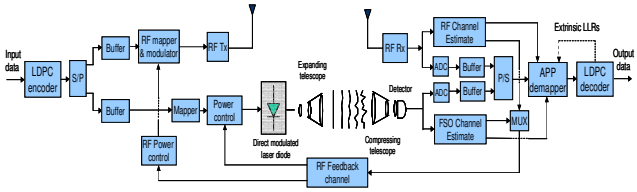

Fig. 1. System model. S/P: serial-to-parallel conversion, LD: laser diode, ADC: A/D converter, P/S parallel-to-serial converter, APP: *a posteriori* probability.

2.2 Wireless channel model

The signal at the RF receiver antenna (see Fig. 1), denoted by $\boldsymbol{s}_k$ can be written as

$$\boldsymbol{s}_k = r_k e^{j\gamma_k} \boldsymbol{c}_k + \boldsymbol{w}_k, \tag{1}$$

where r_k is the fading envelope for kth transmission block, γ_k is the random phase shift occurred during signal transmission of the same block of symbols over a fading channel. The fading at antenna is frequency nonselective, it does not change for the duration of block (slow fading), and it is independent from block to block. The $\boldsymbol{c}_k$ is the vector of transmitted symbols within the kth block. The $\boldsymbol{w}_k$ denotes the block of zero mean circular Gaussian noise samples corresponding to block k.

The corresponding α-μ probability density function (PDF) is given by [8,9]

$$p(r_k) = \frac{\alpha \mu^{\mu} r_k^{\alpha\mu-1}}{\hat{r}^{\alpha\mu}\Gamma(\mu)} \exp\left(-\mu \frac{r_k^{\alpha}}{\hat{r}^{\alpha}}\right), \tag{2}$$

where $\Gamma(.)$ is the Gamma function, and μ>0 is the inverse of the normalized variance of r_t^{α}

$$\mu = \mathrm{E}^2\left\{r_k^{\alpha}\right\} / \mathrm{Var}\left\{r_k^{\alpha}\right\}, \tag{3}$$

where E{.} is the expectation operator, and $\hat{r}$ is a α-root mean value

#113782 - $15.00 USD Received 6 Jul 2009; revised 28 Aug 2009; accepted 10 Sep 2009; published 25 Sep 2009

$$\hat{r} = \sqrt[\alpha]{\mathrm{E}\left\{r_k^{\alpha}\right\}}. \tag{4}$$

The α-μ fading model is employed because Rayleigh, Nakagami-m, exponential, Weibull and one-sided Gaussian distribution functions are all special cases of this model. For example, by setting $\alpha = 2$ and $\mu = 1$ we obtain the Rayleigh distribution, while by setting $\alpha = 2$ and $\mu = 2$ we obtain Nakagami $m = 2$ distribution.

After the signal co-phasing, the resulting signal can be written as

$$\boldsymbol{z}_k = r_k \boldsymbol{c}_k + \boldsymbol{w}_k. \tag{5}$$

2.3 Free-space optical channel model

The FSO communication channel model is described by

$$\boldsymbol{y}_k = R i_k \boldsymbol{x}_k + \boldsymbol{n}_k, \tag{6}$$

where $\boldsymbol{x}_k$ is the kth transmitted block, i_k is the instantaneous intensity gain, $\boldsymbol{y}_k$ is the kth received block of symbols, $\boldsymbol{n}_k$ is the vector of additive white Gaussian noise (AWGN) samples with a normal distribution $N(0,\sigma^2)$ representing the trans-impedance amplifier thermal noise, and R denotes the photodiode responsivity. (Without the loss of generality in the rest of the paper we will set $R = 1$ A/W.) (All signals in (6) are real valued.)

Several PDFs have been proposed for the intensity variations at the receiver side of an FSO link 1. For example, Al-Habash *et al*. [10] proposed a statistical model that factorizes the irradiance as the product of two independent random processes each with a Gamma PDF. It was shown in [1,4,5] that predicted distribution matches very well the distributions obtained from numerical propagation simulations and experiments, and as such is adopted here. The PDF of the intensity fluctuation is given by [1,10]

$$p(i_k) = \frac{2(\alpha'\beta')^{(\alpha'+\beta')/2}}{\Gamma(\alpha')\Gamma(\beta')} i_k^{(\alpha'+\beta')/2-1} K_{\alpha'-\beta'}\left(2\sqrt{\alpha'\beta' i_k}\right),\ i_k > 0 \tag{7}$$

where i_k ($k \geq 0$) is the signal intensity, α' and β' are parameters of the PDF, and $K_{\alpha'-\beta'}(\cdot)$ is the modified Bessel function of the second kind of order α'-β'. The parameters α' and β' are related to the scintillation, and in the case of zero inner scale ($l_0 = 0$) (for plane waves) are given by [1,10]

$$\alpha' = \frac{1}{\exp\left[\dfrac{0.49\sigma_R^2}{(1+1.11\sigma_R^{12/5})^{7/6}}\right]-1}, \qquad \beta' = \frac{1}{\exp\left[\dfrac{0.51\sigma_R^2}{(1+0.69\sigma_R^{12/5})^{5/6}}\right]-1} \tag{8}$$

where σ_R^2 is the Rytov variance [1]

$$\sigma_R^2 = 1.23\ C_n^2\ k^{7/6} L^{11/6}, \tag{9}$$

where $k = 2\pi/\lambda$ (λ is the wavelength), L denotes the propagation distance, and C_n^2 is refractive index structure parameter. Weak fluctuations are associated with $\sigma^2_R<1$, the moderate with $\sigma^2_R \approx 1$, the strong with $\sigma^2_R>1$, and the saturation regime is defined by $\sigma^2_R \to \infty$ [1]. Notice that here we consider the worst case scenario, namely, no aperture averaging is applied.

3. Non-adaptive modulation and coding

In this section we describe the class of large girth quasi-cyclic LDPC codes suitable for use in hybrid FSO-RF transmission (subsection A), and present the numerical results for non-adaptive LDPC-coded modulation (subsection B). Without adaptive modulation and coding, we have to use long interleavers so that neighboring symbols are independent of each other. Although this is not a practical approach for FSO channels, here we use it as the reference case.

#113782 - $15.00 USD Received 6 Jul 2009; revised 28 Aug 2009; accepted 10 Sep 2009; published 25 Sep 2009

3.1 Large girth quasi-cyclic LDPC codes

The LDPC codes under study in this paper belong to the class of quasi-cyclic (QC) LDPC codes [12]. The QC codes, lead to encoder that can be implemented based on shift-registers and modulo-2 adders, while complexity of decoder is low compared to random LDPC codes. The parity-check matrix of LDPC codes considered here can be written in the following form

$$H = \begin{bmatrix} I & I & I & \dots & I \\ I & P^{S[1]} & P^{S[2]} & \dots & P^{S[w_r-1]} \\ I & P^{2S[1]} & P^{2S[2]} & \dots & P^{2S[w_r-1]} \\ \dots & \dots & \dots & \dots & \dots \\ I & P^{(w_c-1)S[1]} & P^{(w_c-1)S[2]} & \dots & P^{(w_c-1)S[w_r-1]} \end{bmatrix}, \qquad (10)$$

where I is qxq (q is a composite number) identity matrix, P is qxq permutation matrix ($p_{i,i+1} = p_{q,1} = 1$, $i = 1,2,\dots,q$-1; other elements of P are zeros), while w_c and w_r represent the number of block-rows and block-columns in (10) (or equivalently column-weight w_c and row-weight w_r of H). The set of integers S are to be carefully chosen from the set $\{0,1,\dots,q\text{-}1\}$ so that the cycles of short length, in corresponding Tanner graph representation of (10) are avoided. The codeword length is $N = |S|q$, where $|S|$ denotes the cardinality of set S, and the code rate is lower bounded by $(1\text{-}w_c/|S|)$.

Example: By selecting $p = 673$ and $S = \{0, 2, 5, 13, 20, 37, 58, 91, 135, 160, 220, 525\}$ an LDPC code of rate 0.75, girth $g = 10$, column weight 3 and length $N = 8076$ is obtained.

The decoding algorithm is based on sum-product with correction term algorithm [13]. The complexity of this algorithm is low and suitable for field-programmable gate array (FPGA) or very-large-scale integration (VLSI) implementation.

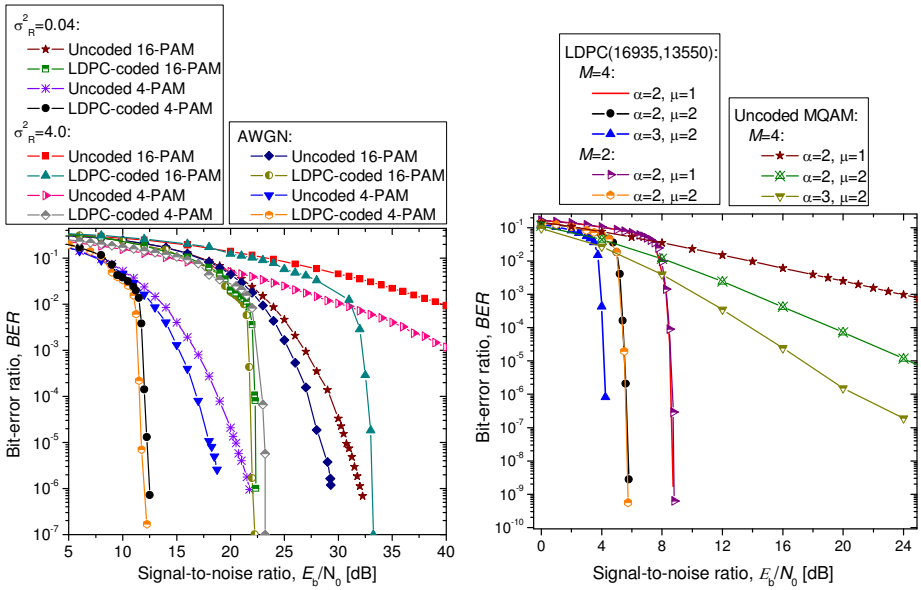

(a) (b)

Fig. 2. Non-adaptive uncoded and LDPC(16935,13550)-coded MQAM and MAPM BERs for: (a) FSO channel, and (b) α-μ wireless fading channel.

#113782 - $15.00 USD Received 6 Jul 2009; revised 28 Aug 2009; accepted 10 Sep 2009; published 25 Sep 2009

3.2 Performance of non-adaptive LDPC-coded modulation

The results of simulations for non-adaptive LDPC(16935,13550)-coded modulation are shown in Fig. 2. The BER plots for MPAM transmission over FSO channel are shown in Fig. 2(a), while BERs for MQAM transmission over α-μ wireless fading channel are shown in Fig. 2(b). In the weak turbulence regime ($\sigma^2_R = 0.04$) the BER performance degradation is small, within 0.5 dB, while in the strong turbulence regime ($\sigma^2_R = 4.0$) the BER performance degradation is so high that adaptive modulation/coding approach described in next two sections is a necessity. From Fig. 2(b) we see that the same LDPC code of high rate provides excellent coding gains for different α-μ wireless fading channels. We also have found that variations for different fading parameters and QPSK are within 4.5 dB at BER of 10^{-7}, while the variations for FSO channel and 4-PAM are within 10.8 dB.

4. Adaptive modulation

In this section we describe different adaptation scenarios suitable for use in hybrid communication system proposed here. There are many parameters that can be varied at the transmitter side relative to the FSO (RF) channel conditions; including data rate, power, coding rate, and combinations of different adaptation parameters. The transmitter power adaptation, can be used to compensate for SNRs variation due to atmospheric turbulence/fading, with the aim to maintain a desired BER in both FSO and RF channels. The power adaptation therefore "inverts" the FSO channel scintillation, and fading in wireless channel so that both FSO and RF channels behave similarly as an AWGN channel. The FSO channel, upon channel inversion, appears to the receiver as standard AWGN channel with $\mathrm{SNR}^{\mathrm{FSO}} = \Gamma_0^{\mathrm{FSO}} / \mathrm{E}\left[1/i_t^2\right]$, where $\Gamma_0^{\mathrm{FSO}} = E_s^{\mathrm{FSO}} / N_0$ is the signal-to-noise ratio in the absence of scintillation, with E_s^{FSO} being the symbol energy and $N_0/2$ being the double-side power spectral density of AWGN related to variance by $\sigma^2 = N_0/2$. Notice that this definition, commonly used in wireless communications [6,7], and also in [3], is different from [1] where SNR is defined as P_o/σ, where $\mathrm{E}[i_t] \le P_o$. The wireless fading channel, upon channel inversion, appears to the receiver as standard AWGN channel with $\mathrm{SNR}^{\mathrm{RF}} = \Gamma_0^{\mathrm{RF}} / \mathrm{E}\left[1/h^2\right]$, where h is channel coefficient, $\Gamma_0^{\mathrm{RF}} = E_s^{\mathrm{RF}} / N_0$ is the signal-to-noise ratio in the absence of fading, with E_s^{RF} being the symbol energy and $N_0/2$ being the double-side power spectral density of AWGN.

In the rest of this section, we derive the optimum power adaptation policy that maximizes the total channel capacity. We further derive the rate adaptation policy but assuming that symbol rates in both channels are fixed, and the symbol rate in RF channel is much smaller than that in FSO channel. As an illustrative example, we assume that MQAM is used in RF channel, while MPAM is used in FSO channel, and determine the spectral efficiency. MPAM is selected because negative amplitude signals cannot be transmitted over FSO channels with direct detection. The MQAM is not power efficient for transmission over FSO channel with direct detection because it requires the addition of DC bias to convert negative amplitudes to positive ones, and as such is not considered here. Notice that M-ary pulse-position modulation (MPPM) can also be used for transmission over FSO channel. Because MPPM is highly spectrally inefficient, we restrict our attention to MPAM instead. Before we continue with the description of different adaptation policies, we have to derive a target bit error probability equations P_b for MPAM and MQAM on an AWGN channel. In MPAM the transmitted signal x takes values from the discrete set $X = \{0,d,\ldots,(M\text{-}1)d\}$ ($M \ge 2$), where d is the Euclidean distance between two neighboring points. If all signal constellation points are equiprobable, the average signal energy is given by $E_s = d^2(M\text{-}1)(2M\text{-}1)/6$, and it is related to the bit energy E_b by $E_s = E_b \log_2 M$, so that signal-to-noise ratio per bit is defined by $SNR_b = E_b/N_0 = E_S/(N_0 \log_2 M) = d^2(M\text{-}1)(2M\text{-}1)/(6N_0 \log_2 M)$. Following the derivation similar to that reported in [6], we derive the following expression for bit error probability of FSO channel:

#113782 - $15.00 USD Received 6 Jul 2009; revised 28 Aug 2009; accepted 10 Sep 2009; published 25 Sep 2009

$$P_b^{\mathrm{MPAM}} \cong \frac{M-1}{M\log_2 M}\operatorname{erfc}\left(\sqrt{\frac{3\Gamma_0^{\mathrm{MPAM}}}{2(M-1)(2M-1)}}\right). \quad (11)$$

were the symbol SNR Γ_0^{MPAM} is the symbol SNR in the absence of scintillation, and erfc(z) function is defined by $\operatorname{erfc}(z)=\left(2/\sqrt{\pi}\right)\int_z^\infty \exp\left(-u^2\right)du.$

Because the Eq. (11) is not invertible, we derive the following empirical formula which is valid in the regime of medium and high signal-to-noise ratios:

$$P_b^{\mathrm{MPAM}} \cong 0.2\exp\left[-\frac{1.85\Gamma_0^{\mathrm{MPAM}}}{2^{2.19\log_2 M}-1}\right]. \quad (12)$$

The corresponding expressions for MQAM are given in [6]. In derivations that follow we will assume that target bit error probabilities in both channels are the same $P_b^{\mathrm{MPAM}} = P_b^{\mathrm{MQAM}} = P_b$. The total spectral efficiency R as the function of bit error probability P_b can be found as

$$R=\frac{1}{2.19}B_{\mathrm{FSO}}\log_2\left(1+K_{\mathrm{FSO}}\Gamma_0^{\mathrm{FSO}}\right)+B_{\mathrm{RF}}\log_2\left(1+K_{\mathrm{RF}}\Gamma_0^{\mathrm{RF}}\right), \quad (13)$$

where $K_{\mathrm{FSO}}=-1.85\backslash\ln\left(5P_b\right)$ and $K_{\mathrm{RF}}=-1.5\backslash\ln\left(5P_b\right)$. Because the total spectral efficiency changes as the channel conditions in either channel change, the spectral efficiency is a function of FSO channel irradiance i_k and RF fading coefficient h as follows

$$R=\frac{1}{2.19}B_{\mathrm{FSO}}\log_2\left(1+K_{\mathrm{FSO}}\Gamma^{\mathrm{FSO}}\left(i_k\right)\frac{P^{\mathrm{FSO}}\left(i_k\right)}{P}\right)+B_{\mathrm{RF}}\log_2\left(1+K_{\mathrm{RF}}\Gamma^{\mathrm{RF}}\left(h\right)\frac{P^{\mathrm{RF}}\left(h\right)}{P}\right), \quad (14)$$

where $\Gamma^{\mathrm{FSO}}\left(i_k\right)=i_k^2\Gamma_0^{\mathrm{FSO}}$ and $\Gamma^{\mathrm{RF}}\left(h\right)=h^2\Gamma_0^{\mathrm{RF}}$. To derive the optimum power adaptation policy, subject to $P^{\mathrm{FSO}}\left(i_k\right)+P^{\mathrm{RF}}\left(h\right)\le P$, we have to define the corresponding Lagrangian, differentiate it with respect to $P^{\mathrm{FSO}}(i_k)$ and $P^{\mathrm{RF}}(h)$ and set corresponding derivatives to be equal to zero. The optimum power adaptation policy is obtained as the result of this derivation:

$$\begin{aligned}\frac{K_{\mathrm{FSO}}P^{\mathrm{FSO}}\left(i_k\right)}{P}&=\begin{cases}\dfrac{1}{\Gamma_{\mathrm{tsh}}}-\dfrac{1}{\Gamma^{\mathrm{FSO}}},\ \Gamma^{\mathrm{FSO}}\ge\Gamma_{\mathrm{tsh}}\\ 0,\ \Gamma^{\mathrm{FSO}}<\Gamma_{\mathrm{tsh}}\end{cases},\quad \Gamma^{\mathrm{FSO}}=\Gamma_0^{\mathrm{FSO}}i_k^2\\ \frac{K_{\mathrm{RF}}P^{\mathrm{RF}}\left(h\right)}{P}&=\begin{cases}\dfrac{1}{\Gamma_{\mathrm{tsh}}}-\dfrac{1}{\Gamma^{\mathrm{RF}}},\ \Gamma^{\mathrm{RF}}\ge\Gamma_{\mathrm{tsh}}\\ 0,\ \Gamma^{\mathrm{RF}}<\Gamma_{\mathrm{tsh}}\end{cases},\quad \Gamma^{\mathrm{RF}}=\Gamma_0^{\mathrm{RF}}h^2\end{aligned} \quad (15)$$

where Γ_{tsh} is the threshold SNR, which is common to both channels. With this adaptation policy more power and higher data rates are transmitted when the FSO (RF) channel conditions are good, less power and lower data rates are transmitted when FSO (RF) channel is bad, and nothing is transmitted when the SNR falls below the threshold Γ_{tsh}. The optimum threshold Γ_{tsh} can be obtained numerically by solving the following equation:

$$\int_{\sqrt{\Gamma_{\mathrm{tsh}}/\Gamma_0^{\mathrm{FSO}}}}^{\infty}\left(\frac{1}{K_{\mathrm{FSO}}\Gamma_{\mathrm{tsh}}}-\frac{1}{K_{\mathrm{FSO}}\Gamma_0^{\mathrm{FSO}}i_k^2}\right)p\left(i_k\right)di_k+b\int_{\sqrt{\Gamma_{\mathrm{tsh}}/\Gamma_0^{\mathrm{RF}}}}^{\infty}\left(\frac{1}{K_{\mathrm{RF}}\Gamma_{\mathrm{tsh}}}-\frac{1}{K_{\mathrm{RF}}\Gamma_0^{\mathrm{RF}}h^2}\right)p\left(h\right)dh=1 \quad (16)$$

#113782 - $15.00 USD Received 6 Jul 2009; revised 28 Aug 2009; accepted 10 Sep 2009; published 25 Sep 2009

where $b = B_{RF}/B_{FSO}$, $p(i_l)$ is the PDF of FSO irradiance i_k given by Eq. (7) and $p(h)$ is the PDF of RF channel coefficient h given by Eq. (2). The optimum spectral efficiency, defined as data rate R over channel bandwidth B, can be evaluated by substituting Eq. (15) into Eq. (14) to obtain:

$$\frac{R}{B}=\frac{1}{2.19}\int_{\sqrt{\Gamma_{tsh}/\Gamma_0^{FSO}}}^{\infty}\log_2\left(\frac{\Gamma_0^{FSO}i_k^2}{\Gamma_{tsh}}\right)p\left(i_k\right)di_k+b\int_{\sqrt{\Gamma_{tsh}/\Gamma_0^{RF}}}^{\infty}\log_2\left(\frac{\Gamma_0^{RF}h^2}{\Gamma_{tsh}}\right)p\left(h\right)dh\ [\text{bits/s/Hz}] \quad (17)$$

Although this adaptive-rate adaptive-power scheme provides excellent spectral efficiencies, the optimum threshold computation in Eq. (16) is time extensive. Instead, we can perform the truncated channel inversion with fixed rate. The truncated channel inversion adaptation can be performed by

$$\frac{P^{FSO}\left(i_k\right)}{P}=\begin{cases}\dfrac{1}{i_k^2E_{\Gamma_{tsh}}^{FSO}\left[1/i_k^2\right]}, & \Gamma^{FSO}\geq\Gamma_{tsh}\\ 0, & \Gamma^{FSO}<i_{tsh}\end{cases}\qquad\frac{P^{RF}\left(h\right)}{P}=\begin{cases}\dfrac{1}{h^2E_{\Gamma_{tsh}}^{RF}\left[1/h^2\right]}, & \Gamma^{RF}\geq\Gamma_{tsh}\\ 0, & \Gamma^{RF}<\Gamma_{tsh}\end{cases} \quad (18)$$

where

$$E_{\Gamma_{tsh}}^{FSO}\left[\frac{1}{i_k^2}\right]=\int_{\sqrt{\Gamma_{tsh}/\Gamma_0^{FSO}}}^{\infty}\frac{p\left(i_k\right)}{i_k^2}di_k,\ E_{\Gamma_{tsh}}^{RF}\left[\frac{1}{h^2}\right]=\int_{\sqrt{\Gamma_{tsh}/\Gamma_0^{RF}}}^{\infty}\frac{p\left(h\right)}{h^2}dh\,. \quad (19)$$

The threshold Γ_{tsh} in Eq. (18) is obtained by maximizing the spectral efficiency as given below

$$\begin{aligned}R=\max_{\Gamma_{tsh}}\Bigg\{&\frac{1}{2.19}B_{FSO}\log_2\left(1+K_{FSO}\Gamma_0^{FSO}\frac{1}{E_{\Gamma_{tsh}}^{FSO}\left[1/i_k^2\right]}\right)P\left(i_k\geq\sqrt{\Gamma_{tsh}/\Gamma_0^{FSO}}\right)\\&+B_{RF}\log_2\left(1+K_{RF}\Gamma_0^{RF}\frac{1}{E_{\Gamma_{tsh}}^{RF}\left[1/h^2\right]}\right)P\left(h\geq\sqrt{\Gamma_{tsh}/\Gamma_0^{RF}}\right)\Bigg\}\end{aligned} \quad (20)$$

where

$$P\left(i_k\geq\sqrt{\Gamma_{tsh}/\Gamma_0^{FSO}}\right)=\int_{\sqrt{\Gamma_{tsh}/\Gamma_0^{FSO}}}^{\infty}p\left(i_k\right)di_k\qquad P\left(h\geq\sqrt{\Gamma_{tsh}/\Gamma_0^{RF}}\right)=\int_{\sqrt{\Gamma_{tsh}/\Gamma_0^{RF}}}^{\infty}p\left(h\right)dh \quad (21)$$

In Fig. 3 we show the spectral efficiencies for FSO system only, which can be achieved using the optimum power and rate adaptation and MPAM for different target bit error probabilities, and both: (a) weak turbulence regime ($\sigma^2_R = 0.04$, $\alpha' = 51.913$, $\beta' = 49.113$), and (b) strong turbulence regime ($\sigma^2_R = 4$, $\alpha' = 4.3407$, $\beta' = 1.3088$). For example, the spectral efficiency R/B of 2 bits/s/Hz at $P_b = 10^{-9}$ is achieved for symbol SNR of 23.3 dB in weak turbulence regime, and 26.2 dB in strong turbulence regime. In the same Figure we report the spectral efficiencies that can be achieved by both channel inversion ($\Gamma_{tsh} = 0$) and truncated channel inversion ($\Gamma_{tsh}>0$). In the weak turbulence regime (see Fig. 3(a)) even simple channel inversion performs comparable to optimum adaptive-power adaptive-rate scheme. However, in the strong turbulence regime (see Fig. 3(b)) this scheme faces significant performance degradation. On the other hand, the truncated channel inversion scheme in strong turbulence regime faces moderate performance degradation, about 3.7 dB at $P_b = 10^{-9}$ for spectral efficiency of 2 bits/s/Hz. The optimum adaptation policy for FSO channel at $P_b = 10^{-6}$ for

#113782 - $15.00 USD Received 6 Jul 2009; revised 28 Aug 2009; accepted 10 Sep 2009; published 25 Sep 2009

spectral efficiency 4 bits/s/Hz provides moderate improvement of 3.3 dB in the weak turbulence regime over non-adaptive scheme, while the improvement in the strong turbulence regime is significant 31.7 dB.

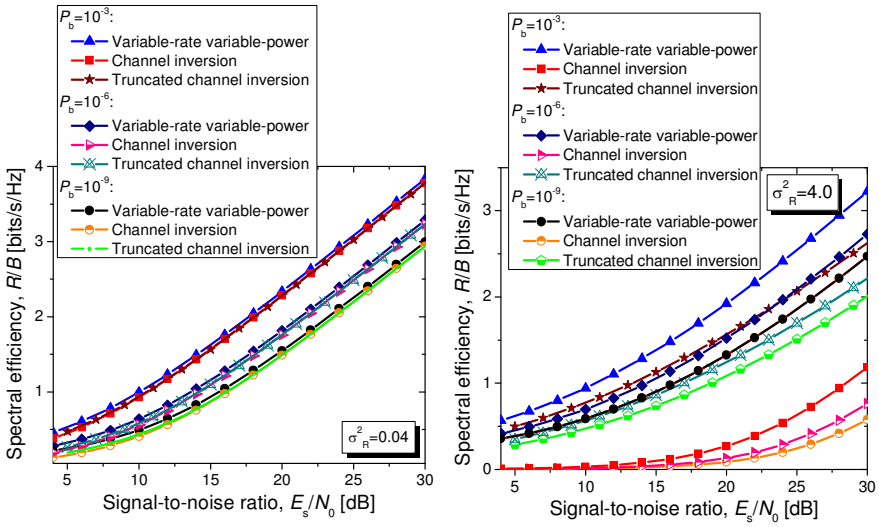

Fig. 3. Spectral efficiencies of FSO system against symbol SNR for different target bit probabilities of error: (a) in weak turbulence regime, and (b) in strong turbulence regime.

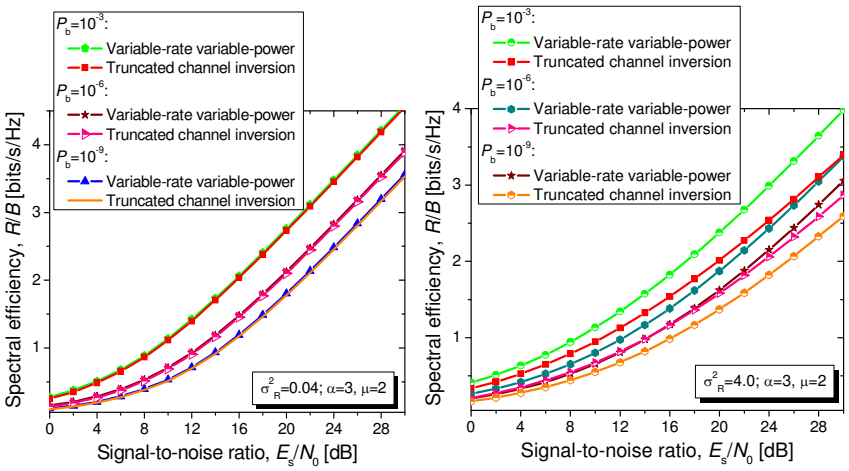

Fig. 4. Spectral efficiencies of hybrid FSO-RF system with α = 3, μ = 2 fading against symbol SNR for different target bit probabilities of error: (a) in weak turbulence regime, and (b) in strong turbulence regime.

#113782 - $15.00 USD Received 6 Jul 2009; revised 28 Aug 2009; accepted 10 Sep 2009; published 25 Sep 2009

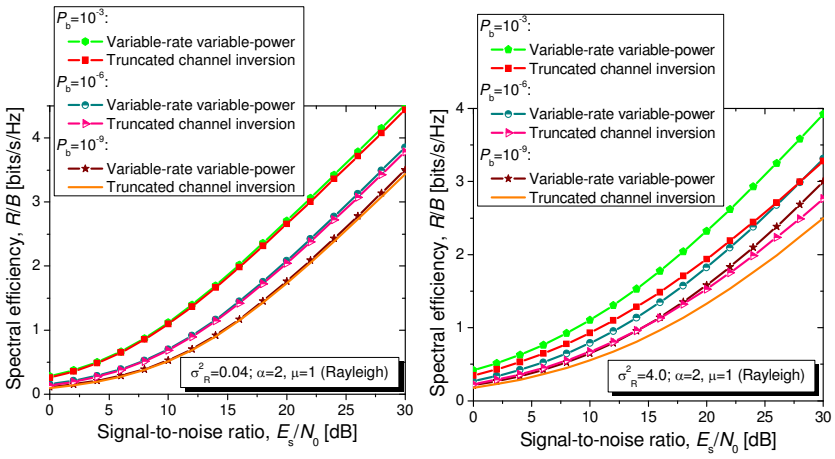

Fig. 5. Spectral efficiencies of hybrid FSO-RF system with α = 2, μ = 1 (Rayleigh) fading against symbol SNR for different target bit probabilities of error: (a) in weak turbulence regime, and (b) in strong turbulence regime.

In Fig. 4 we report the spectral efficiencies for hybrid FSO-RF system shown in Fig. 1, with RF sub-system fading parameters α = 3, μ = 2 in both weak turbulence regime (Fig. 4(a)) and strong turbulence regime (Fig. 4(b)). We assume that FSO subsystem symbol rate is 10 times larger than RF subsystem data rate, that is b = 0.1. For spectral efficiency of 2 bits/s/Hz the hybrid FSO-RF system outperforms the FSO system by 3.39 dB at BER of 10^{-6} and 3.49 dB at BER of 10^{-9}. It is interesting to notice that even truncated channel inversion for hybrid system outperforms the optimum adaptation of FSO system by 0.8 dB at BER of 10^{-9} and spectral efficiency of 2 bits/s/Hz.

In Fig. 5 we report the spectral efficiencies for hybrid FSO-RF system, with RF sub-system fading parameters α = 2, μ = 1 (corresponding to Rayleigh fading) in both weak turbulence regime (Fig. 5(a)) and strong turbulence regime (Fig. 5(b)). This case corresponds to the situation where there is no line-of-site between transmit and receive antennas for RF subsystem. We again assume that b = 0.1. For spectral efficiency of 2 bits/s/Hz the hybrid FSO-RF system outperforms the FSO system by 3.01 dB at BER of 10^{-6} and 3.11 dB at BER of 10^{-9}. The truncated channel inversion for hybrid system performs comparable to the optimum adaptation of FSO system.

In this section we described two different adaptive modulation scenarios for both FSO system with RF feedback and hybrid FSO-RF system. In next section we describe the adaptive coding based on coded modulation.

5. Adaptive coded modulation

By using the trellis coded modulation (TCM) or cosset codes, we can separate the encoding and modulation process (see [6,7] for more details). However, to keep the complexity of this approach reasonably low the convolutional or block codes should be simple and short. Those codes are in principle of low rate and weak so that coding gains are moderate. For example, the adaptive coding scheme based on TCM proposed in [7] is about 5 dB away from channel capacity. Instead, in this paper we propose to implement adaptive coding based on LDPC-coded modulation. For FSO system, the input data are LDPC encoded and written to a buffer. Based on FSO channel irradiance, i_t, $\log_2 M(i_t)$ bits are taken at a time from a buffer and used to select the corresponding point from MPAM signal constellation. For hybrid FSO-RF system, the LDPC encoded sequence is split between FSO and RF subsystem (see Fig. 1). To facilitate the implementation we assume that symbol rates in both subsystems are fixed while constellation sizes and emitted powers are determined based on channel conditions in both

#113782 - $15.00 USD Received 6 Jul 2009; revised 28 Aug 2009; accepted 10 Sep 2009; published 25 Sep 2009

channels using the adaptation scenarios described in previous section. We further assume that symbol rate in RF subsystem is at least 10 times lower than that in FSO subsystem (e.g., 1 Giga symbol/s in FSO subsystem and 100 Mega symbol/s in RF subsystem).

The code rate adaptation can be achieved by varying different parameters in (10). To simplify implementation and resolve the synchronization problems related to the variable symbol rate transmission, we propose to keep the codeword length (symbol rate) fixed, but vary the permutation-block P size and row weight in (10) instead. We designed rate-adaptive QC LDPC code of codeword length 28800 (that is shorter than turbo-product code proposed by Mizuochi *et al*. [14]), with possible rates {0.875, 0.84, and 0.8}, whose BER performance is shown in Fig. 6. Even highest rate code (0.875) outperforms the turbo-product code of rate 0.82, and significantly outperforms the concatenated RS code.

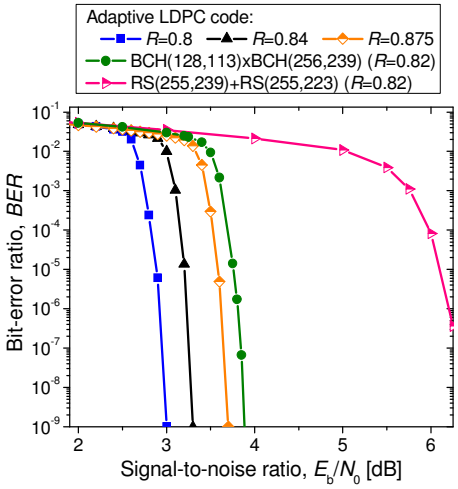

Fig. 6. BER performance of adaptive LDPC code for QPSK with Gray mapping.

In Fig. 7(a) we show R/B performance of FSO system with adaptive LDPC-coded MPAM for different adaptation scenarios. Given the fact that the channel capacity of FSO channel under atmospheric turbulence is an open problem, we show in the same figure an *upper bound* in the absence of atmospheric turbulence from [15]. The coding gain over adaptive modulation at $P_b = 10^{-6}$ for R/B = 4 bits/s/Hz is 7.2 dB in both (weak and strong) turbulence regimes. Larger coding gains are expected at lower BERs, and for higher spectral efficiencies. Further improvements can be obtained by increasing the girth of LDPC codes, and employing better modulation formats. The increase in codeword length to 100,515 does not improve R/B performance that much as shown in Fig. 7(a). It is interesting to notice that by employing adaptive coding, the communication under saturation regime is possible, as shown in Fig. 7(a). Moreover, for variable-rate variable-power scheme there is no degradation in saturation regime compared to strong turbulence regime. Overall improvement from adaptive modulation and coding for R/B = 4 bits/s/Hz at $P_b = 10^{-6}$ over non-adaptive uncoded modulation ranges from 10.5 dB (3.3 dB from adaptive modulation and 7.2 dB from coding) in the weak turbulence regime to 38.9 dB in the strong turbulence regime (31.7 dB from adaptive modulation and 7.2 dB from coding).

In Fig. 7(b) we show R/B performance of hybrid FSO-RF system with adaptive LDPC-coded modulation (MPAM is used in FSO subsystem and MQAM in RF subsystem) for different adaptation scenarios. The symbol rate in FSO subsystem is set to be 10 times larger than that in RF subsystem (b = 0.1). For spectral efficiency of 4 bits/s/Hz at BER of 10^{-6}, the improvement of hybrid FSO-RF system over FSO system is 5.25 dB in Rayleigh fading (α = 2, μ = 1), 5.51 dB in Nakagami m = 2 fading (α = 2, μ = 2) and 5.63 dB in α = 3, μ = 2 fading. For spectral efficiency of 2 bits/s/Hz at the same BER, the improvement of hybrid FSO-RF

#113782 - $15.00 USD Received 6 Jul 2009; revised 28 Aug 2009; accepted 10 Sep 2009; published 25 Sep 2009

system over FSO system is 3.32 dB in Rayleigh fading, 3.72 dB in Nakagami $m = 2$ fading and 3.86 dB in $\alpha = 3$, $\mu = 2$ fading.

Notice that results presented here are universal; they are applicable for any combination of propagation length L, wavelength λ, and structure parameter C^2_n, as long as L is much longer than λ, so that the geometrical optics approximation by (9) holds. In practice, the refractive index structure parameter C^2_n varies from about 10^{-17} $m^{-2/3}$ for very weak turbulence to about 10^{-12} $m^{-2/3}$ for strong turbulence [1]. For example, a value of $\sigma^2_R = 4$ can be obtained with $C^2_n = 8 \times 10^{-14}$ $m^{-2/3}$, $L = 1065$ m, and $\lambda = 780$ nm.

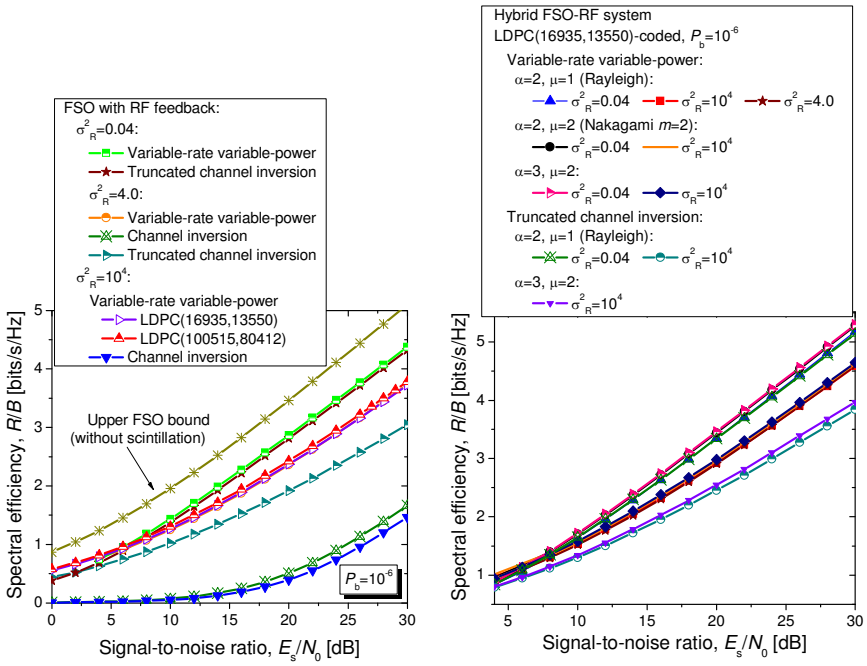

(a) (b)

Fig. 7. Spectral efficiencies against symbol SNR for adaptive LDPC-coded modulation: (a) FSO with RF feedback only, and (b) hybrid FSO-RF system.

6. Conclusions

We described a hybrid FSO-RF system suitable for transmission at high rates and proposed two adaptation policies: (i) optimum variable-rate and variable-power adaptation scheme, and (ii) truncated channel inversion scheme. The optimum adaptation scheme is derived by maximizing the total channel capacity. The proposed scheme outperforms FSO optimum adaptation scheme by 3.39 dB at BER of 10^{-6} and spectral efficiency of 2 bits/s/Hz, for the strong atmospheric turbulence in FSO channel and for Rayleigh fading in RF channel. With LDPC coding, the proposed scheme outperforms corresponding LDPC-coded FSO scheme at BER of 10^{-6} in the strong atmospheric turbulence for $R/B = 4$ bits/s/Hz as follows: 5.25 dB in Rayleigh RF fading, 5.51 dB in Nakagami $m = 2$ RF fading and 5.63 dB in $\alpha = 3$, $\mu = 2$ RF fading. With proposed adaptive coding scheme even communication in saturation regime is possible. We also report the spectral efficiencies for proposed hybrid FSO-RF system with adaptive modulation/coding and compare them against FSO system.

Topics of interest in future research include: (i) determination of improvements in hybrid channels when channel state information (CSI) is imperfect and (ii) estimation of degradation due to delay in delivery of CSI to transmitter.

#113782 - $15.00 USD Received 6 Jul 2009; revised 28 Aug 2009; accepted 10 Sep 2009; published 25 Sep 2009

Acknowledgments

This work was supported in part by the National Science Foundation (NSF) under Grant IHCS-0725405.

#113782 - $15.00 USD Received 6 Jul 2009; revised 28 Aug 2009; accepted 10 Sep 2009; published 25 Sep 2009